J Mater Sci: Mater Electron (2017) 28:3272–3277
DOI 10.1007/s10854-016-5919-x

# Effect of TWEEN 80 on the morphology and antibacterial properties of ZnO nanoparticles

V. Rajendar[1,4] · C. H. Shilpa Chakra[2] · B. Rajitha[3] · K. Venkateswara Rao[2] · M. Chandra Sekhar[1] · B. Purusottam Reddy[1] · Si-Hyun Park[1]

Received: 15 August 2016 / Accepted: 18 October 2016 / Published online: 24 October 2016


**Abstract** Globule shaped nanoparticles of zinc oxide were prepared using a simple solution combustion method in the presence of TWEEN 80. The nanoparticles were 80 ± 20 nm in size with a hexagonal Wurtzite structure. Fourier transform infrared spectroscopy analysis of the samples showed the presence of no impurities. The size of the nanoparticles decreased with increasing concentration of TWEEN 80, peaking at a concentration of 0.05 M, above which the particle sized started to increase again. The antibacterial studies conducted on all of the samples revealed the superior activity of the zinc oxide nanoparticles prepared using the highest concentration of TWEEN 80.

## 1 Introduction

Zinc oxide (ZnO) nanoparticles represent a classic example of omnipotent nanoparticles with their seemingly endless list of applications [1–6]. Furthermore, the preparation of ZnO nanoparticles is facile and does not require sophisticated instrumentation to prepare a plethora of shapes and sizes. ZnO is a room temperature crystalline material and is considered safe for use on humans. Due to these exceptional qualities, ZnO nanoparticles have been used for catalytic [7], thermoelectric [8], photocatalytic [9], solar [6, 10, 11], cancer therapy [12–15], antibacterial [16, 17], and antiviral applications [18, 19]. ZnO nanoparticles have been prepared by multiple techniques, such as the co-precipitation, sol–gel [20, 21], microwave assisted [22], green chemistry [23, 24], flame transport [25–27], and solution combustion synthesis [28, 29] methods. Of these methods, solution combustion synthesis requires the lowest amount of resources and only a little experience in carrying out the synthesis process. However, the control of the particle size and shape during this process is tedious and requires the use of toxic surfactants, polymers or other stabilizing agents.

TWEEN 80 is a cheap, biocompatible and easy to use surfactant polysorbate that is used in multiple drugs and is generally regarded as safe (GRAS) for human use [30]. Although the use of TWEEN 80 for the preparation of ZnO has been studied on multiple occasions [31, 32], its application to the solution combustion method has not been greatly discussed. This lack of use of TWEEN 80 may be due to the low stability of micelles in a heated environment.

In this paper, we propose a new mechanism for the solution combustion synthesis of ZnO nanoparticles using TWEEN 80. The role of the concentration of TWEEN 80 in reducing the particle size of the nanoparticles is also discussed. Further, the antimicrobial properties of the prepared nanoparticles were tested on four different bacterial species.

## 2 Materials and methods

### 2.1 Materials

All of the materials mentioned in the manuscript were purchased from Alfa Aesar unless otherwise indicated. All of the chemicals were used as-purchased and were not

✉ Si-Hyun Park
sihyun_park@ynu.ac.kr

[1] Department of Electronic Engineering, Yeungnam University, Gyeongsan-si, Gyeongsangbuk-do 38541, Republic of Korea

[2] Centre for Nano Science and Technology, Jawaharlal Nehru Technological University Hyderabad, Hyderabad, India

[3] Department of Physics, BVRIT Hyderabad College of Engineering for Women, JNTUH, Hyderabad, India

[4] Department of Physics, B.V. Raju Institute of Technology, Narsapur, Medak, Telangana, India

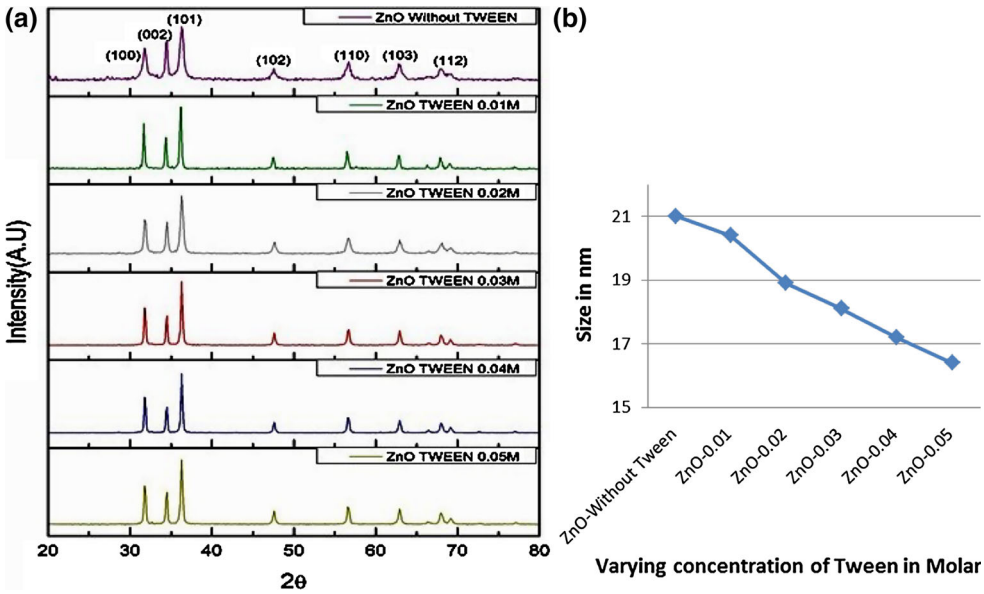


**Fig. 1** Structural analysis of all of the ZnO nanoparticles (**a**) 2D XRD Plot of Zinc Oxide Nanoparticles with and without TWEEN 80 (**b**) Decrease in crystallite size with increasing concentration of TWEEN 80

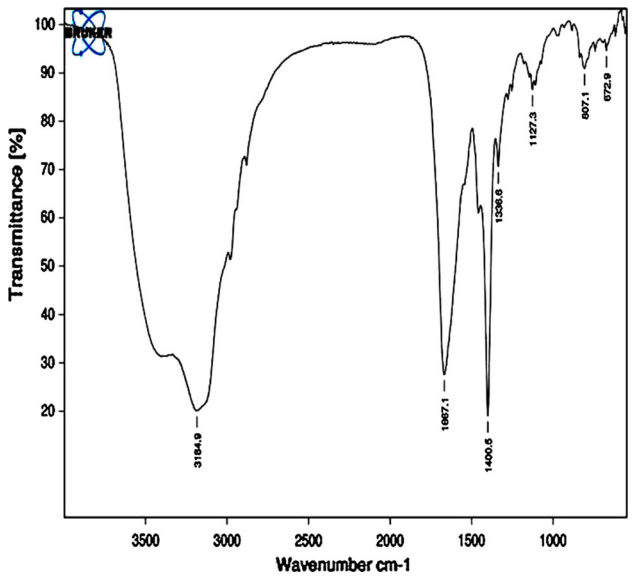


**Fig. 2** FTIR Spectra of Zinc Oxide nanoparticles

subjected to any additional purification. De-Ionized (DI) water was used as the solvent in all of the reactions.

## 2.2 Synthesis of ZnO nanoglobules

In a typical synthesis, 0.05 M Zinc acetate was mixed with 0.01 M Dextrose solution in the presence of TWEEN 80 ($C_6H_{124}O_{26}$) (0.01–0.05 M). The solution was made up to 50 mL with DI water and mixed thoroughly for 30 min. The resulting cloudy solution was then subjected to a solution combustion process similar to those mentioned in earlier reports. Briefly, 50 mL of the cloudy solution was poured into a glass beaker and placed inside a muffle furnace (CEM, USA, PHOENIX AIRWAVE) and heated to 250 °C. Due to the presence of Dextrose, the sample spontaneously ignites and the resulting deflagration corresponds to the formation of ZnO nanoparticles. Five reactions with different concentrations of TWEEN 80 (0.01, 0.02, 0.03, 0.04, 0.05 M) were conducted using this procedure. The synthesized materials were analyzed using X-ray diffraction (XRD) (Bruker AXS D8 Advance), Fourier transform infrared spectroscopy (FTIR) (FT-IR, Magna Nicolet 550), Scanning electron microscopy (SEM) with energy dispersive X-ray spectroscopy (EDS), XL30, Philips microscope, and transmission electron microscopy (TEM) with small angle electron diffraction (SAED) (JEOL JEM 2100 - 200 kV).

## 2.3 Antibacterial studies

The antibacterial and antifungal activities of the ZnO nanoparticles were analyzed by the well diffusion method. Their effects on both gram positive (*S. aureus* and *B. subtilis*) and gram negative (*E.coli*) bacteria, along with a fungal strain (*C.albicans*), were studied by a standard protocol mentioned in other papers. Briefly, petri-dishes were washed and sterilized in an autoclave before nutrient agar medium was poured into them and allowed to solidify in a laminar air flow chamber. Using a sterile cotton swab, fresh bacterial cultures with known colony forming units were streaked to obtain uniform growth. Six wells with a diameter of 5 mm were cut into the agar plates using a sterile cork borer before they were loaded with six different concentrations (0.02, 0.04, 0.06, 0.08, 0.1 and 0.12 mg/μL) of ZnO-TWEEN 0.08 solution. The plates were incubated for 12 h at 37 °C and the zone of inhibition was recorded by measuring the diameter of the inhibition zone around the well.

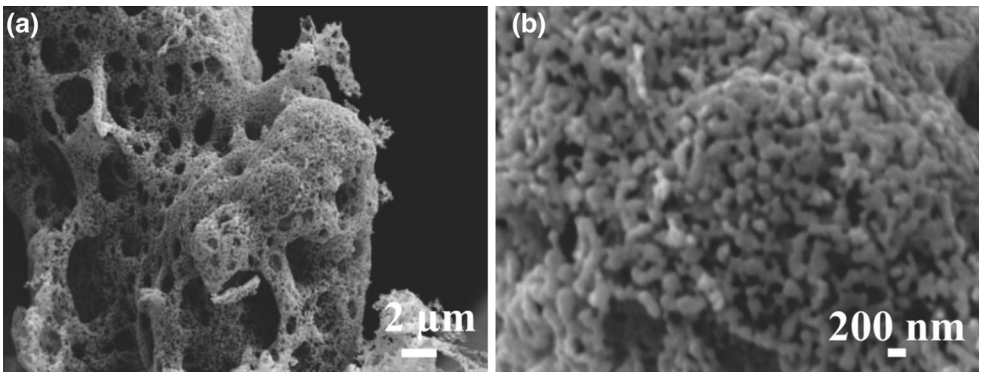


**Fig. 3** Morphology of ZnO Nanoparticles prepared using 0.05 M TWEEN 80 **a** Low Magnification, **b** High Magnification

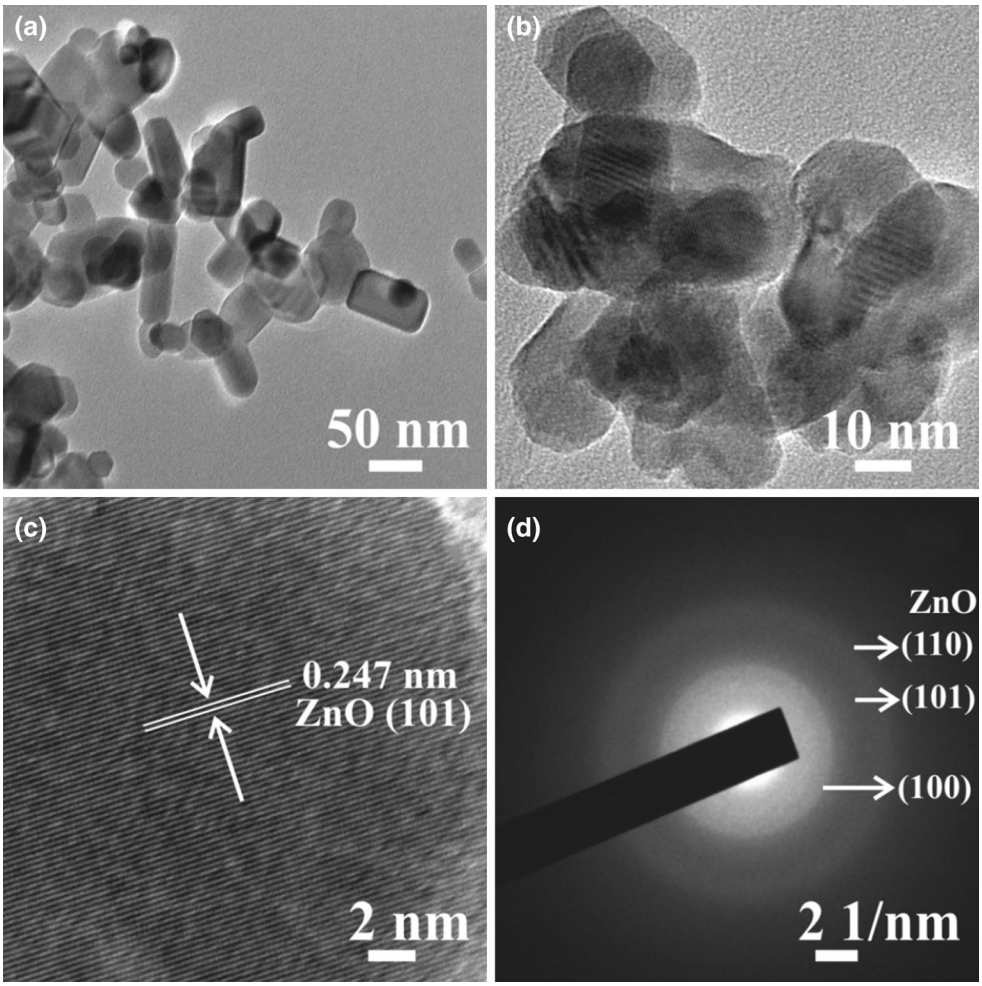


**Fig. 4** **a**, **b** TEM images, **c** d-spacing, **d** SAED Patterns of ZnO Nanoparticles using 0.05 M TWEEN 80

## 3 Results and discussion

### 3.1 XRD

The diffractograms from all of the samples can be seen in Fig. 1a. It is clearly evident from the XRD data that all of the samples consisted of single phase ZnO hexagonal wurtzite crystals corresponding to JCPDS#36-1451. However, the crystallite sizes of the samples (determined by the Scherrer equation) decreased with increasing concentration of TWEEN 80 (Fig. 1b). It is interesting to note here that, although TWEEN 80 would be degraded in the solution combustion process, the formation of smaller crystallites is a direct indication of its involvement in the synthesis process. The formation of smaller crystallites could be due to the formation of more nucleation sites

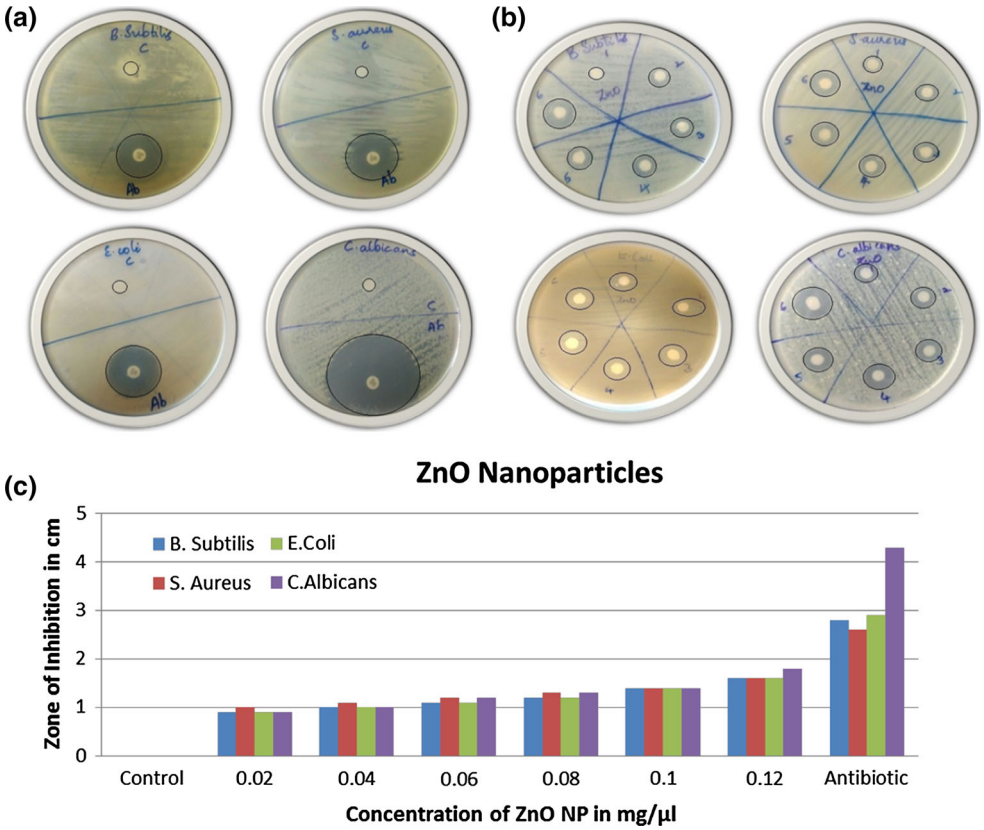


**Fig. 5** Antimicrobial activity of the ZnO nanoglobules prepared using 0.05 M TWEEN80. **a** Positive and negative control for measuring the zone of inhibition, **b** Antimicrobial activity of ZnO nanoglobules at various concentrations, **c** Diameter of the zone of inhibition for different concentrations of ZnO nanoglobules

during the 30 min incubation process prior to combustion in the presence of TWEEN 80. Figure 1b shows the linear decrease in the crystallite size from 21 to 16 nm with increasing concentration of TWEEN 80. Furthermore, the X-ray reflections become much stronger and narrower with increasing surfactant concentration, which befits the explanation given above.

### 3.2 FTIR

To further understand the role of TWEEN 80 in the synthesis process, the FTIR spectra of all of the samples were recorded. The FTIR patterns for all of the samples were similar and a representative graph is shown in Fig. 2. From the FTIR study, we were able to record the presence of organic groups in the sample through the presence of C–H bending, C–O and C–C stretching vibrations at wave numbers of 500–800, 1336, 1123 and 1400 $cm^{-1}$, respectively. It is fascinating to see that although the samples were subjected to a high temperature combustion process, organic residues from TWEEN 80 were present on the nanoparticles. This vindicates the XRD result which revealed a decrease in the crystallite sizes of the samples with increasing TWEEN 80 concentration.

### 3.3 Morphology and elemental analysis

As the ZnO prepared using 0.05 M TWEEM 80 had the lowest crystallite size, these samples were used for further characterization. The particle size of these samples were analyzed using both SEM and TEM and the related images can be seen in Figs. 3 and 4. From the SEM results, it can be seen that the samples are globule or tear drop shaped within a size range of 80–120 nm. These values were confirmed by TEM analysis, in which the particle size was determined to be 80–100 nm. However, it is important to note that all of the nanoparticles are joined via a cloudy aura around them in the TEM images. This could be due to the presence of a thin ZnO layer joining all of the nanoparticles together. These layers are formed due to the high temperatures reached during the solution combustion method, fusing the adjacent nanoparticles together. The particle size distribution analysis conducted using the TEM measurements also confirmed their size to be in the range of 80–100 nm. Elemental analysis of the samples showed the presence of Zn, O and C, revealing their high purity.

Closer observation of the nanoparticles using TEM revealed the d-spacing between the atomic layers of ZnO to be 0.247 nm, which corresponds closely to ZnO JCPDS#36-1451. The corresponding SAED patterns of the

samples relate to hexagonal Wurtzite crystals of ZnO. The particles distribution and SAED results can be seen in Fig. 4a and d, respectively.

### 3.4 Antimicrobial properties of ZnO nanoglobules

Mechanism of antibacterial activity includes physical and chemical process. By physical means ZnO NPs destroys and damages the bacterial cell membrane, resulting in a leakage of cytoplasmic contents. Through chemical process increase the reactive oxygen species (ROS), by enhancing oxidative stress mechanism. From both the process bacterial cell burst due to the release of intracellular content and finally death of cell occurs [33]. The antimicrobial activity of a selected sample of ZnO prepared using 0.05 M TWEEN 80 was studied in gram positive, gram negative and fungal strains and the results can be seen in Fig. 5. The degree of bacterial inhibition was seen to be in direct correlation with the concentration of ZnO globules. Furthermore, it was interesting to observe that the gram negative bacterial strains were more susceptible to inhibition through ZnO than their gram positive counterparts. Further, *C.albicans* exhibited a higher degree of inhibition, which was similar to that observed for the gram negative bacteria. Also, the inhibition of the fungal strain was seen to be higher in the positive control where an antibiotic was used. ZnO is a semiconducting material which is known to produce surface super oxides when irradiated with light with a wavelength greater than its band gap. These surface super oxides eventually lead to the formation of reactive oxygen species when in water, leading to the structural damage of any organic material in its vicinity. This process has been well studied and has been applied to target bacteria, fungi and cancer cells. A quantitative analysis of the zones of inhibition can be seen in Fig. 5, which directly represents the antimicrobial efficacy of the ZnO nanoglobules.

## 4 Conclusions

ZnO nanoglobules with an average diameter of 80 nm were prepared via solution combustion synthesis. The samples were prepared in a two-step process where the zinc precursor was allowed to react with various concentrations of TWEEN 80 for a brief amount of time before being subjected to ignition. The combustion process resulted in the formation of globule shaped nanoparticles. Structural characterization of the samples showed hexagonal Wurtzite crystals typical of ZnO, with the crystallite size of the samples decreasing with increasing TWEEN 80 concentration. The FTIR results showed the presence of organic molecules along with ZnO, confirming the role of TWEEN 80 in the formation process of the nanoglobules. Antimicrobial studies conducted on the nanoglobules formed using 0.05 M TWEEN 80 showed their good inhibitory action on gram positive and gram negative bacteria, as well as on fungal strains.

**Acknowledgments** The authors are graceful to the department of Electrical Engineering, Yeungnam University, Republic of Korea, Centre for Nano Science and Technology, Jawaharlal Nehru Technological University, Hyderabad, India and BV Raju Institute of Technology, Narasapur, Medak, India for providing the research facilities to undertake this work.

## References

1. P.J.P. Espitia, N.F.F. Soares, J.S.R. Coimbra, N.J.D. Andrade, R.S. Cruz, E.A.A. Medeiros, Food Bioprocess Technol. **5**(5), 1447–1464 (2012)
2. C. Klingshirn, J. Fallert, H. Zhou, J. Sartor, C. Thiele, F.M. Flaig, D. Schneider, H. Kalt, Phys. Status Solidi B **247**(6), 1424–1447 (2010)
3. G.J. Nohynek, J. Lademann, C. Ribaud, M.S. Roberts, Crit. Rev. Toxicol. **37**(3), 251–277 (2007)
4. K. Schilling, B. Bradford, D. Castelli, E. Dufour, J.F. Nash, W. Pape, S. Schuttle, I. Tooley, J.Y.D. Bosch, F. Schellauf, Photochem. Photobiol. Sci **9**(4), 495–509 (2010)
5. Z.L. Wang, Mater. Sci. Eng. R **64**(3–4), 33–71 (2009)
6. R. Yu, Q. Lin, S. Leung, Z. Fan, Nano Energy **1**(1), 57–72 (2012)
7. R.M. Mohamed, D.L. McKinney, W.M. Sigmund, Mater. Sci. Eng. R **73**(1), 1–13 (2012)
8. J. He, Y. Liu, R. Funahashi, J. Mater. Res. **26**(15), 1762–1772 (2011)
9. J. Liqiang, S. Xiaojun, S. Jing, C. Weimin, X. Zili, D. Yaoguo, Sol. Energy Mater. Sol. Cells **79**(2), 133–151 (2003)
10. L. Li, T. Zhai, Y. Bando, D. Golberg, Nano Energy **1**(1), 91–106 (2012)
11. Q. Zhang, C.S. Dandeneau, X. Zhou, C. Cao, Adv. Mater. **21**(41), 4087–4108 (2009)
12. C. Hanley, J. Layne, A. Punnoose, K.M. Reddy, I. Coombs, A. Coombs, K. Feris, D. Wingett, Nanotechnology **19**(29), 295103 (2008)
13. W. Hu, Y. Liu, H. Yang, X. Zhou, C.M. Li, Biosens. Bioelectron. **26**(8), 3683–3697 (2011)
14. J. Li, D. Guo, X. Wang, H. Wang, H. Jiang, B. Chen, Nanoscale Res. Lett. **5**(6), 1063–1071 (2010)
15. S. Nair, A. Sasidharan, V.V. Divya Rani, D. Menon, S. Nair, K. Manzoor, S. Raina, J. Mater. Sci. Mater. Med **20**(Suppl 1), S235–S241 (2009)
16. V. Rajendar, B. Rajitha, T. Dayakar, C.H. Shilpa Chakra, K. Venkateswara Rao, Rend. Fis. Acc. Lincei. **27**, 521–531 (2016)
17. V. Rajendar, T. Dayakar, K. Shobhan, I. Srikanth, K. Venkateswara Rao, Superlattices Microstruct **75**, 551–563 (2014)
18. Y. Jang, J. Park, Y.K. Pak, J.J. Pak, J. Nano. Sci. Nano. technol **12**(7), 5173–5177 (2012)
19. Y.K. Mishra, R. Adelung, C. Rohl, D. Shukla, F. Spors, V. Tiwari, Antivir Res. **92**(2), 305–312 (2011)
20. S.M.H. Hejazi, F. Majidi, M.P. Tavandashti, M. Ranjbar, Mater. Sci. Semicond. Process. **13**(4), 267–271 (2010)
21. M.A. Tshabalala, B.F. Dejene, H.C. Swart, Phys. Rev. B Condens. Matter **407**(10), 1668–1671 (2012)
22. N. Uma Sangari, S. Chitra Devi, J. Solid State Chem. **197**, 483–488 (2013)
23. K.D. Bhatte, D.N. Sawant, D.V. Pinjari, A.B. Pandit, B.M. Bhanage, Mater. Lett. **77**, 93–95 (2012)

24. A.C. Janaki, E. Sailatha, S. Gunasekaran, Spectrochim. Acta Part A **144**, 17–22 (2015)
25. J. Grottrup, I. Paulowicz, A. Schuchardt, V. Kaidas, S. Kaps, O. Lupan, R. Adelung, Y.K. Mishra, Ceram. Int. **42**(7), 8664–8676 (2016)
26. Y.K. Mishra, G. Modi, V. Cretu, V. Postica, O. Lupan, T. Reimer, I. Paulowicz, W. Benecke, L. Kienle, R. Adelung, A.C.S. Appl, Mater. Interfaces **7**(26), 14303–14316 (2015)
27. T. Reimer, I. Paulowicz, R. Roder, S. Kaps, O. Lupan, S. Chemnitz, W. Benecke, C. Ronning, R. Adelung, Y.K. Mishra, A.C.S. Appl, Mater. Interfaces **6**(10), 7806–7815 (2014)
28. F.A. Deorsola, D. Vallauri, J. Mater. Sci. **46**(3), 781–786 (2011)
29. C. Lin, C. Hwang, J. Chin. Chem. Soc. **55**(6), 1266–1271 (2008)
30. B.A. Kerwin, J. Pharm. Sci. **97**(8), 2924–2935 (2008)
31. Y. Khan, S.K. Durrani, M. Mehmood, J. Ahmad, M.R. Khan, S. Firdous, Appl. Surf. Sci. **257**(5), 1756–1761 (2010)
32. M.Z. Hussain, R. Khan, R. Ali, Y. Khan, Mater. Lett. **122**, 147–150 (2014)
33. V. Lakshmi Prasanna, R. Vijayaraghavan, Langmuir **31**(33), 9155–9162 (2015)